Supplementary Figures

Figure S16. Prognostic outcome of each molecular subclass from Decipher retrospective cohort via Kaplan-Meier analysis for metastasis (MET)-free survival rates.

Figure S17. Prognostic outcome difference between late events of *PTEN* and *CHD1* deletions, and early events of *ERG* fusion and *SPOP* mutation via Kaplan-Meier analysis for biochemical recurrence (BCR) free and prostate cancer specific mortality (PCSM) free survival rates.

Figure S18. Pathological outcome difference between late events and early events in Decipher retrospective cohort (n=1,626) via univariable analyses.

Figure S19. Pathological outcome difference between late events and early events in Decipher prospective cohort (n=6,532) via univariable analyses.

Figure S20. Alluvial diagrams of Gleason scores, lymph node invasion status and tumor stages from TCGA cohort.

Figure S21. Correlation of gene set enrichment output between lymph node invasion and tumor lineages: similar signaling pathways between lymph node invasion and *ERG*/*PTEN* lineage (from the “early” to “late” state), but divergent pathways between lymph node invasion and *SPOP*/*CHD1* lineage.

Figure S22. Divergent signaling pathways in *SPOP*/*CHD1* lineage, when compared to lymph node invasion and *ERG*/*PTEN* lineage.

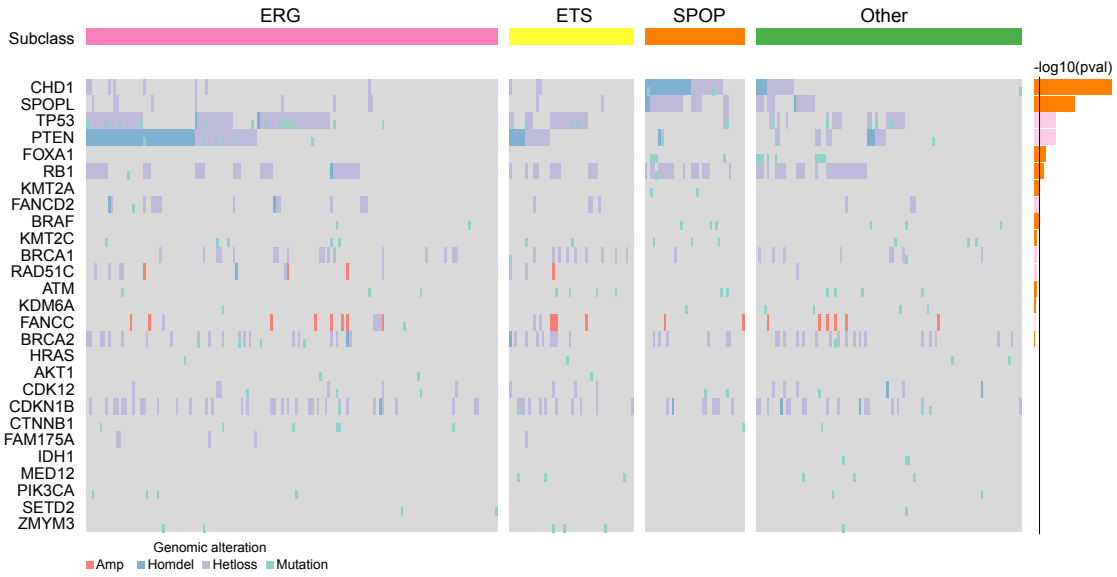

Figure S1. Different enrichment of recurrent genomic alterations in *ERG* fusion and *SPOP* mutant subclasses from TCGA localized prostate cancer cohort. Different colors represent genomic alterations. The alteration enrichment between two subclasses was calculated by two-sided Fisher's exact test. Orange color denotes the enrichment in *SPOP* mutant subclass and pink color denotes the enrichment in *ERG* fusion subclass.

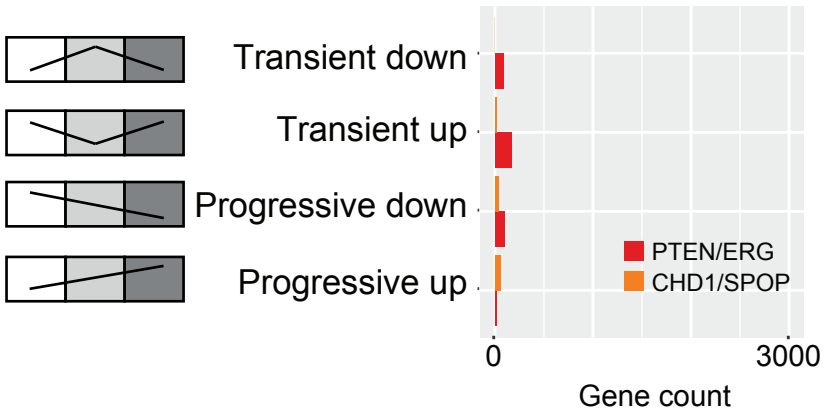

Figure S2. Number of progressively and transiently upregulated and downregulated genes from normal to *ERG* fusion with *PTEN* deletion and *ERG* fusion without *PTEN* deletion (red), or from normal to *SPOP* mutation with *CHD1* deletion and *SPOP* mutation without *CHD1* deletion (orange).

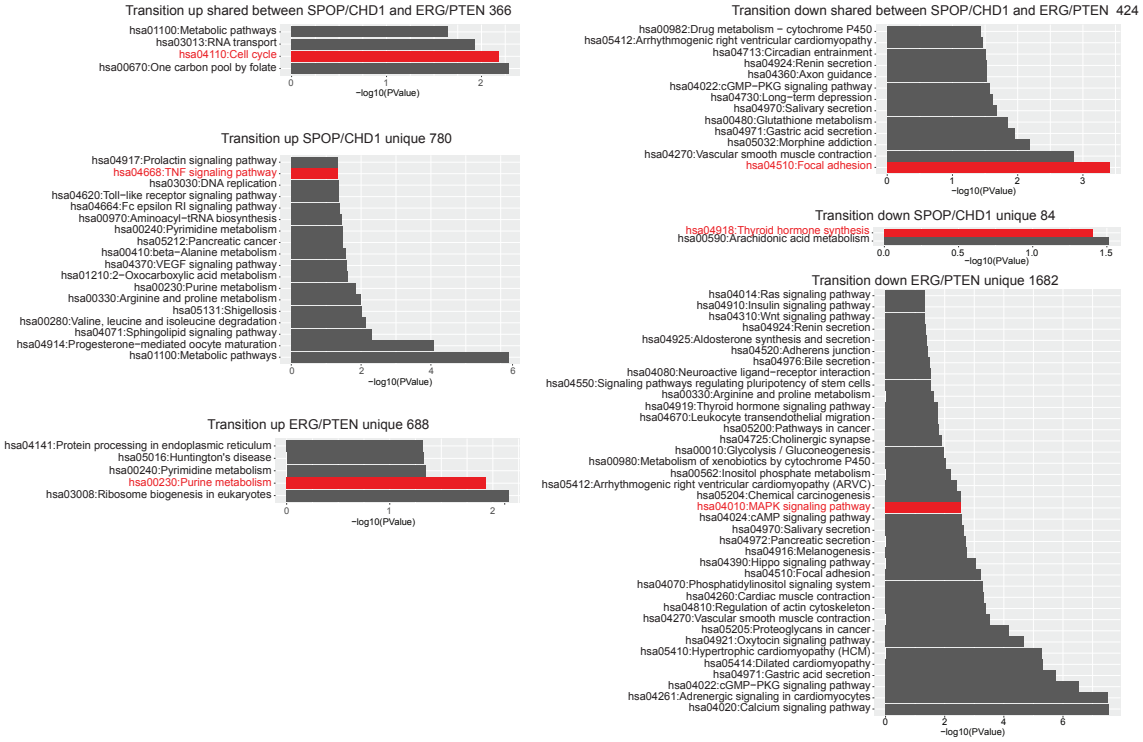

Figure S3. Enriched signaling pathways of shared and uniquely altered genes between two tumor lineage models: *ERG*/*PTEN* and *SPOP*/*CHD1*. The red color denotes the examples of similar enriched pathway found in mouse models.

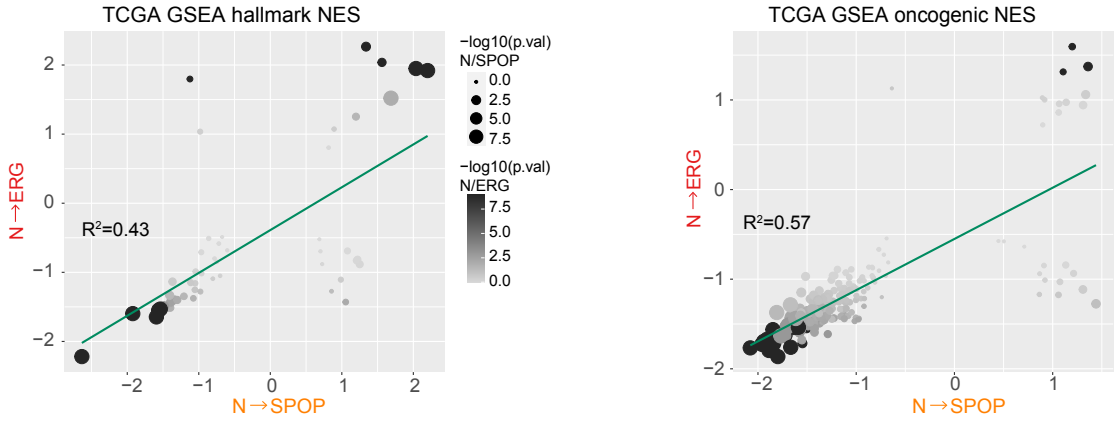

Figure S4. Similar gene set enrichment output from normal to early progression events between two tumor lineage models in TCGA cohort. NES represents normalized enrichment score from GSEA output.

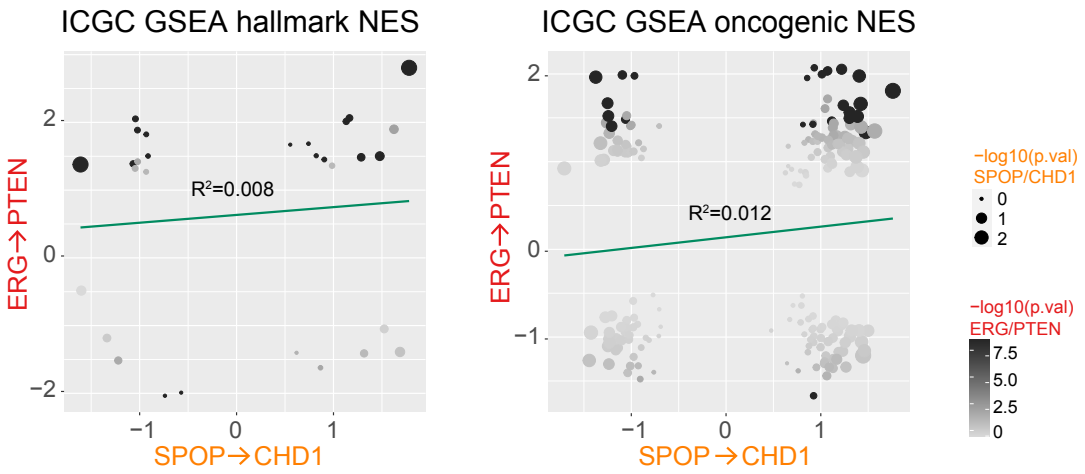

Figure S5. Divergent gene set enrichment output from early to late progression events between two tumor lineage models in ICGC cohort. NES represents normalized enrichment score from GSEA output.

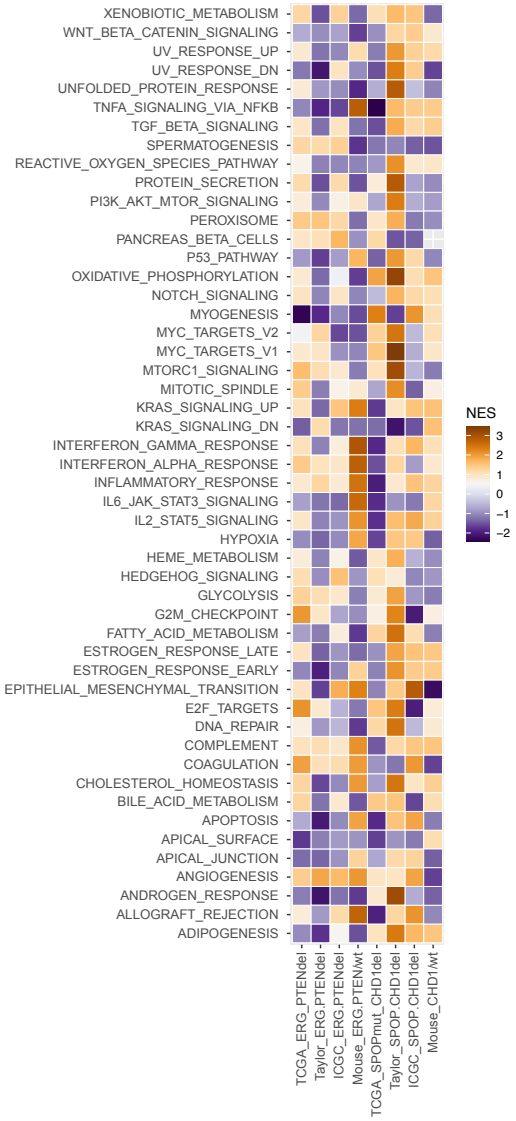

Figure S6. Gene Set Enrichment Analysis (GSEA) output from early to late progression events in TCGA, Taylor, ICGC human patient cohorts, *ERG*/*PTEN* mouse tissue and *CHD1* mouse organoid samples.

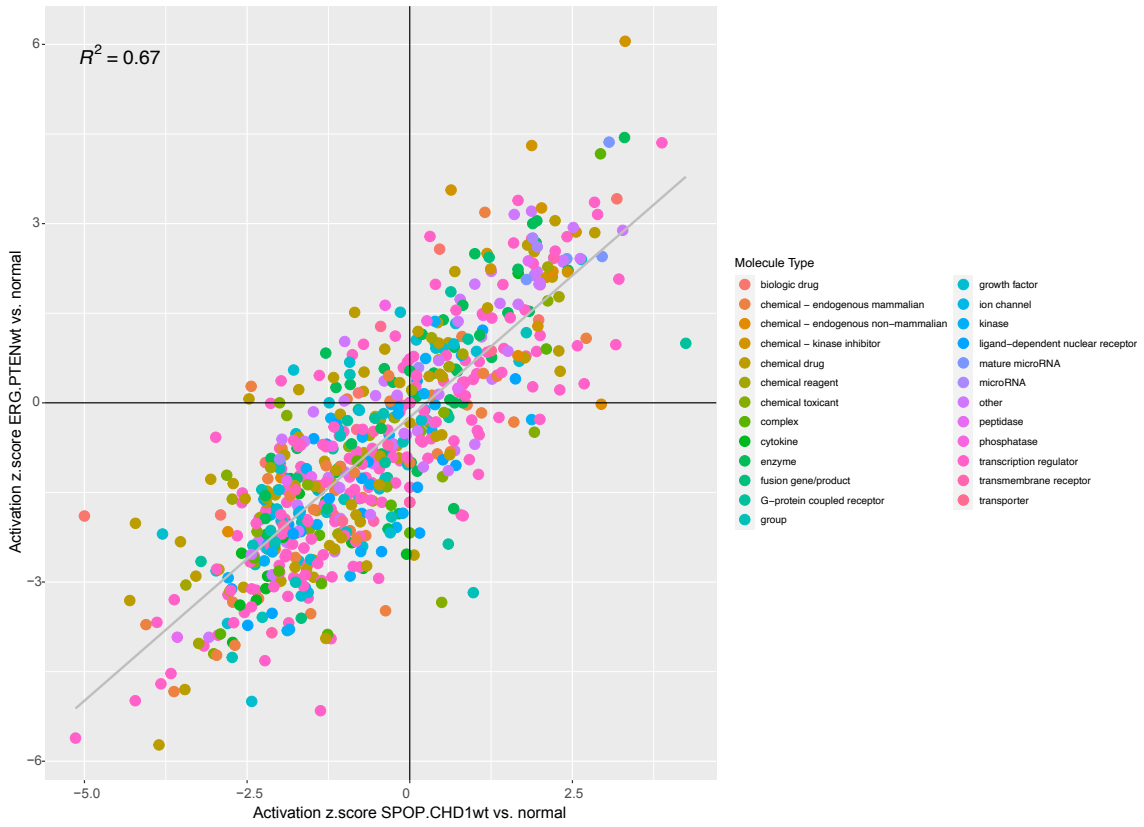

Figure S7. Similar predicted upstream regulators from normal to early progression events between two tumor lineage models in TCGA cohort.

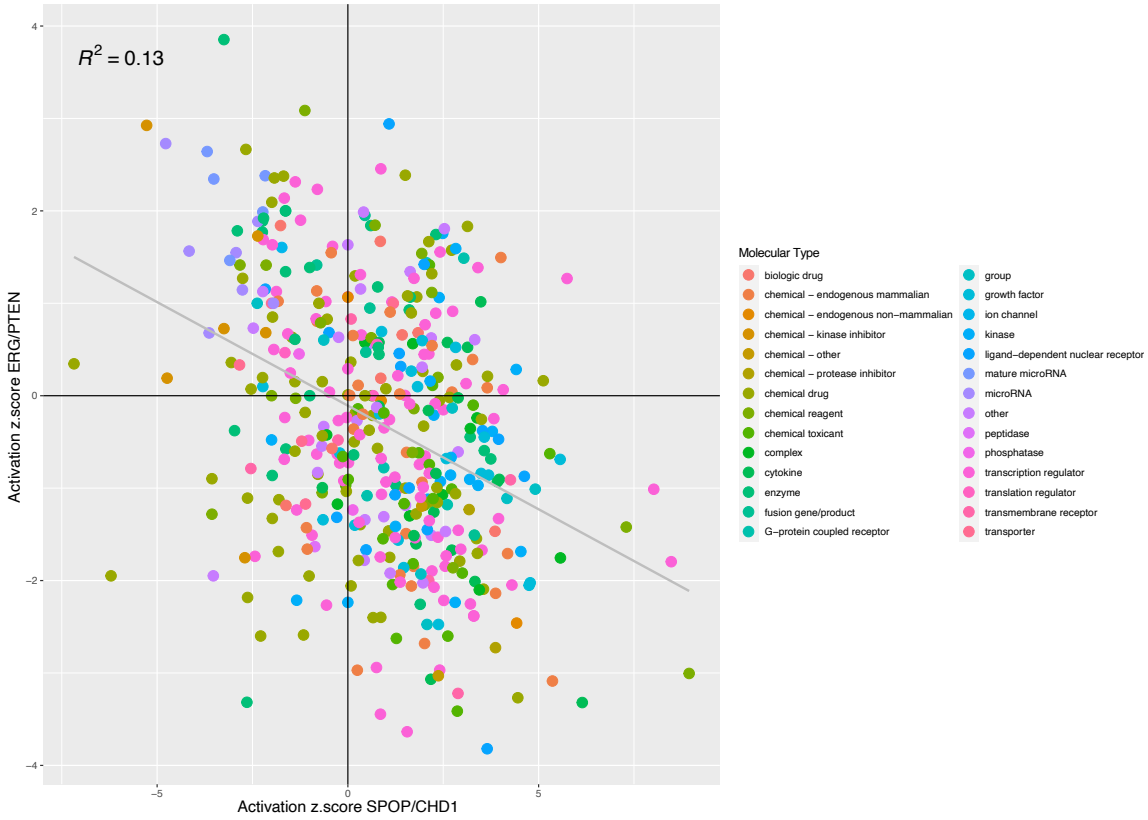

Figure S8. Different predicted upstream regulators from early to late progression events between two tumor lineage models in Taylor cohort.

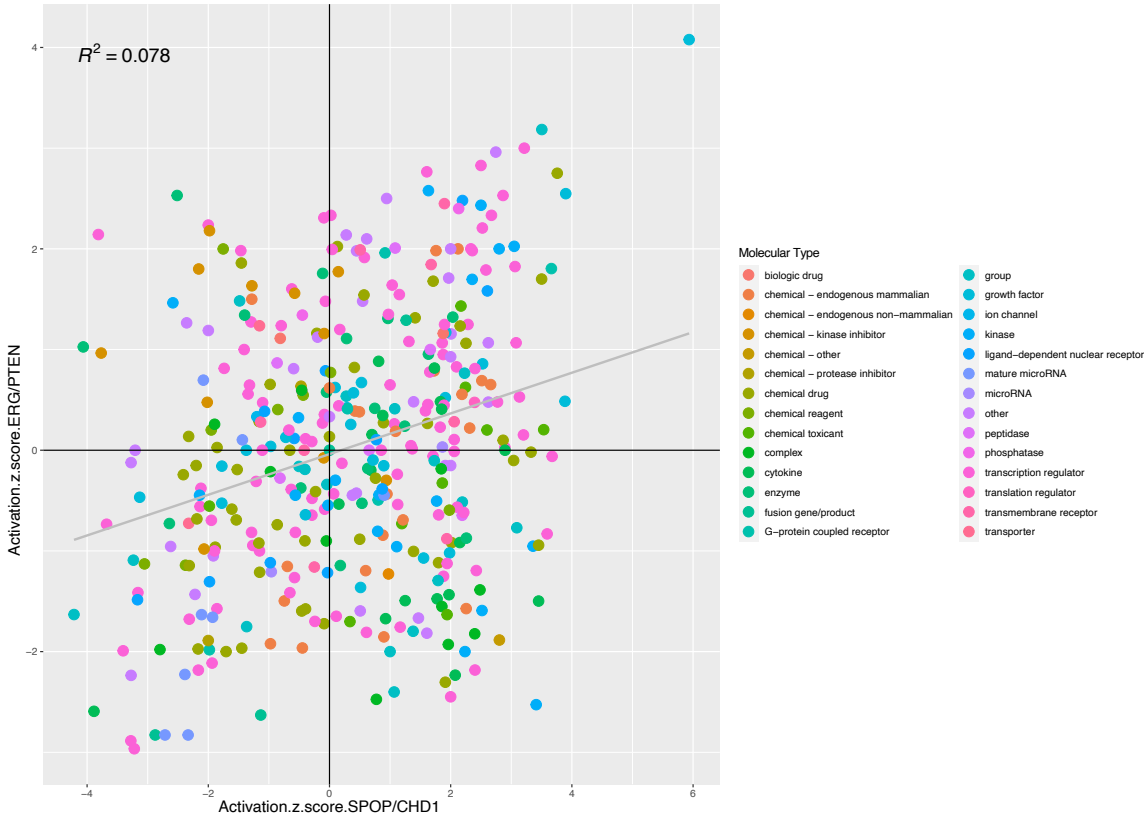

Figure S9. Different predicted upstream regulators from early to late progression events between two tumor lineage models in ICGC cohort.

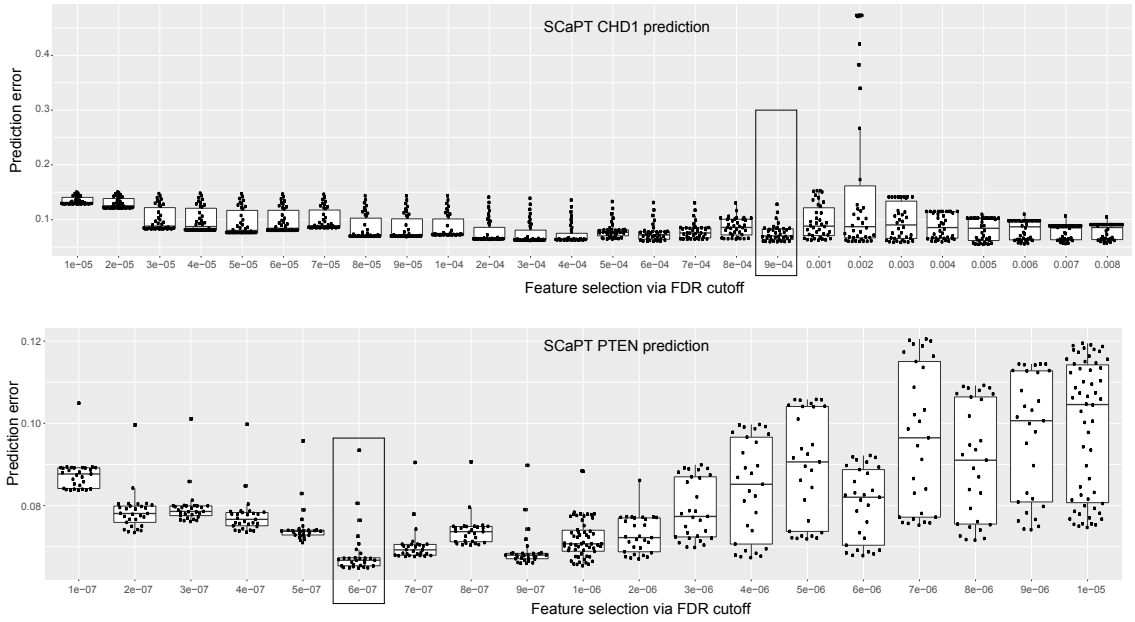

Figure S10. SCaPT models performance of *PTEN* and *CHD1* prediction via 10-fold cross validation based on different feature and cost parameter from SVM model.

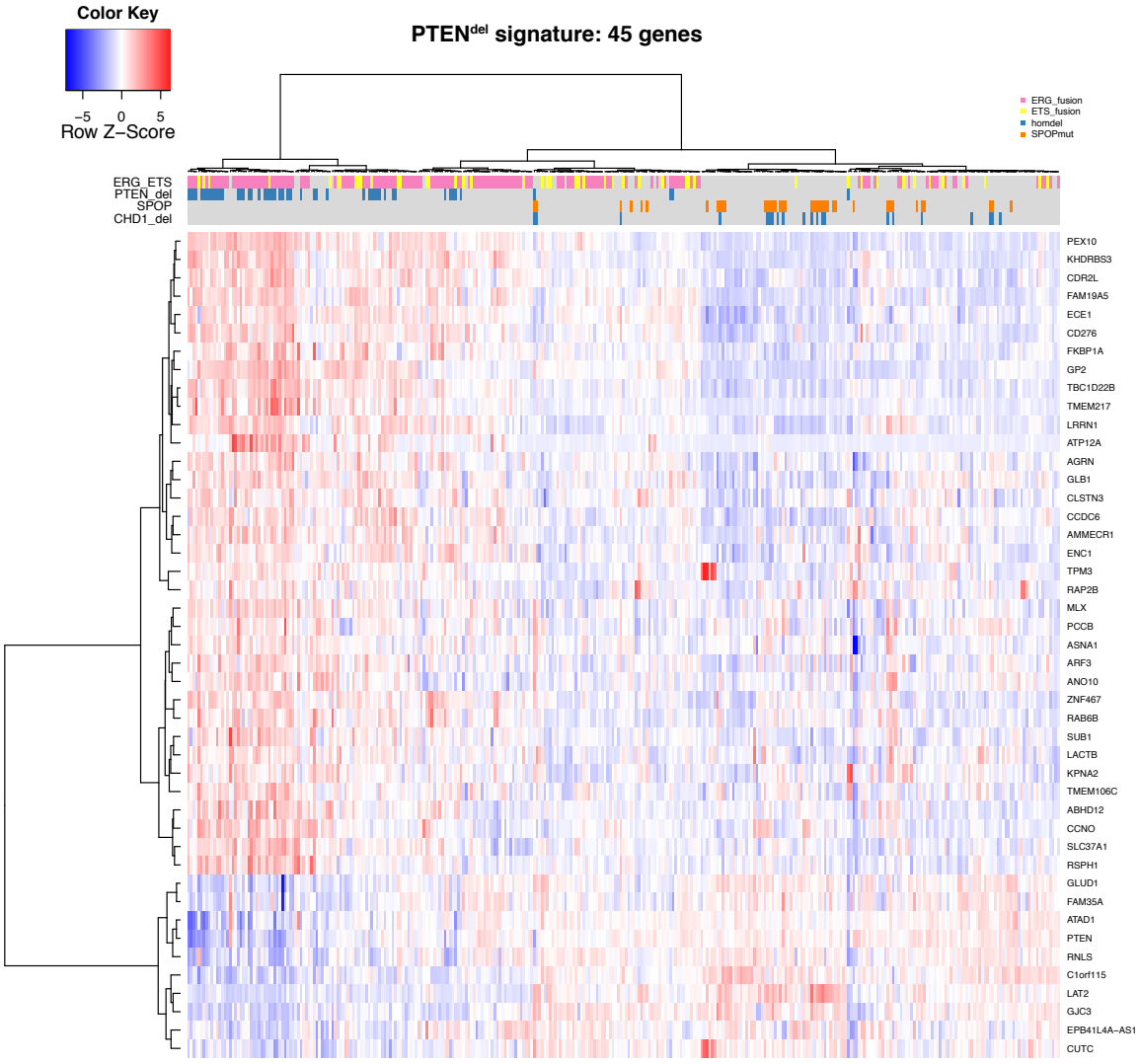

Figure S11. Significant enrichment of corresponding *PTEN* deleted cases on the basis of unsupervised hierarchical clustering, based on *PTEN*^{del} signature.

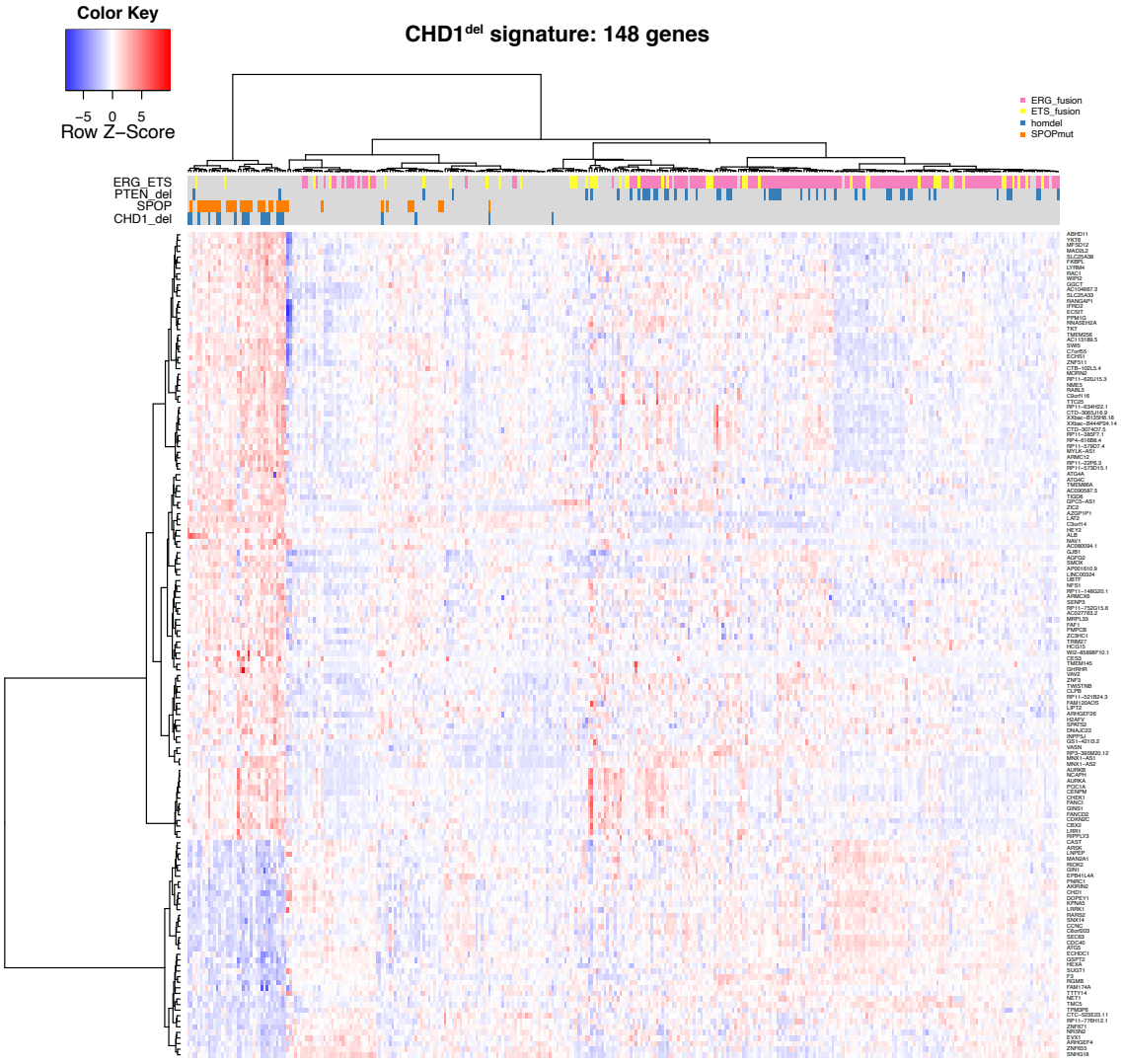

Figure S12. Significant enrichment of corresponding *CHD1* deleted cases on the basis of unsupervised hierarchical clustering, based on *CHD1*^{del} signature.

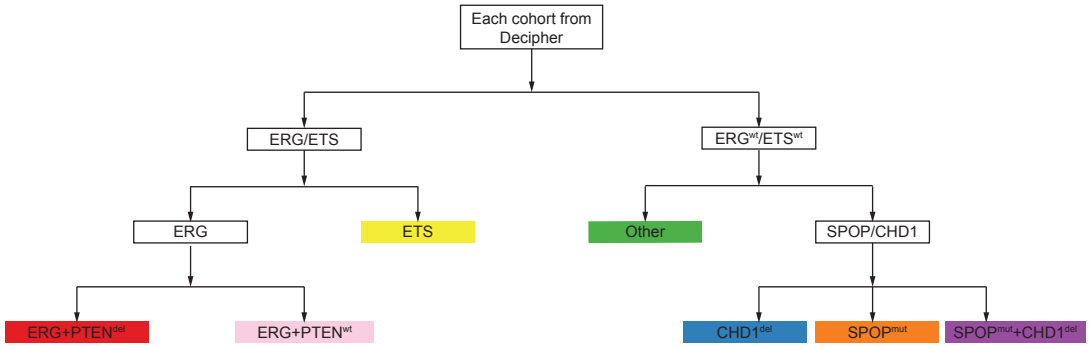

Figure S13. Decision tree for classifying molecular subclass on Decipher cohorts.

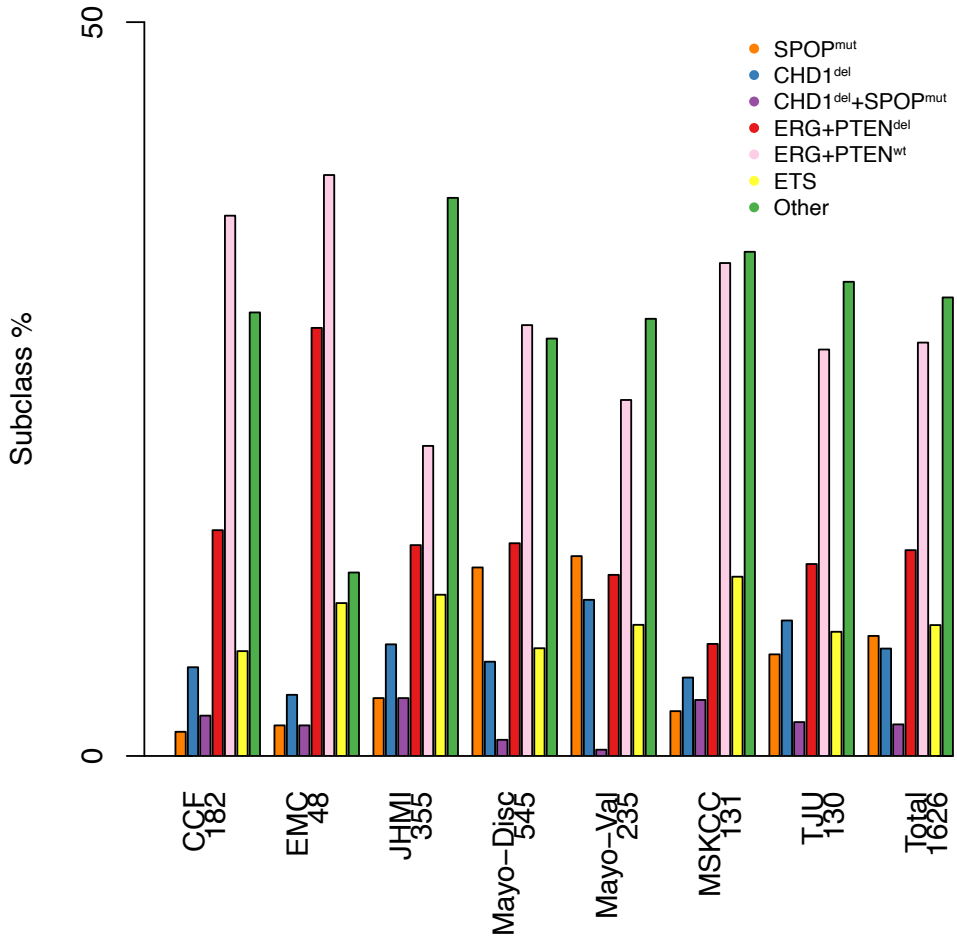

Figure S14. Proportion of each molecular subclass from individual study of Decipher retrospective cohort with 1,632 samples, on the basis of SCaPT models and decision tree.

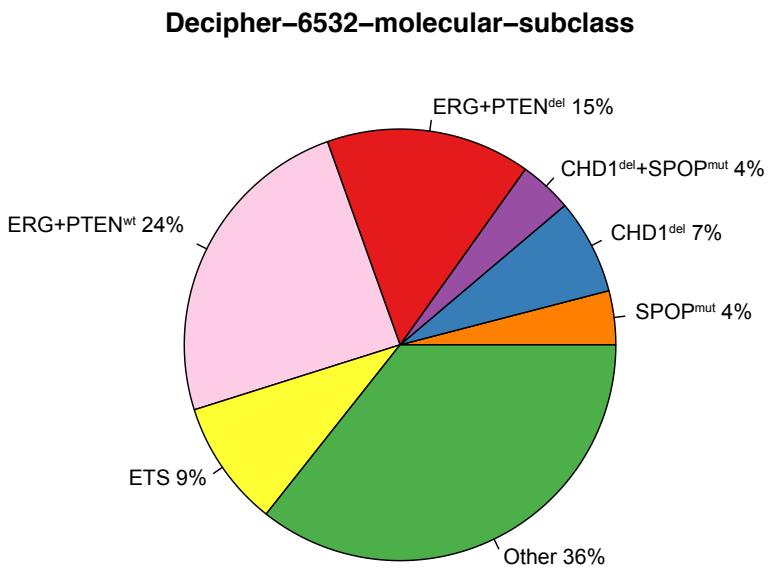

Figure S15. The pie chart of classified subclasses from the Decipher prospective cohort with 6,532 samples, on the basis of SCaPT models and decision tree.

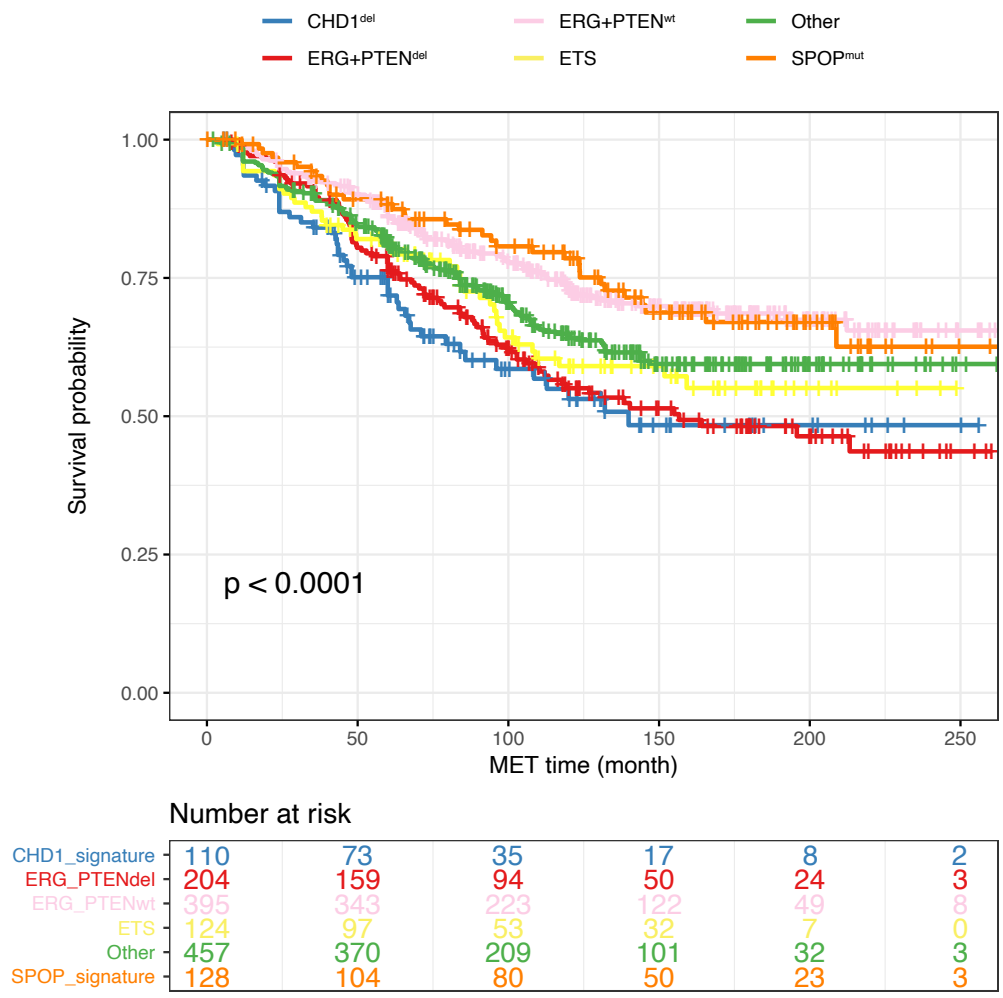

Figure S16. Prognostic outcome of each molecular subclass from Decipher retrospective cohort via Kaplan-Meier analysis for metastasis (MET)-free survival rates.

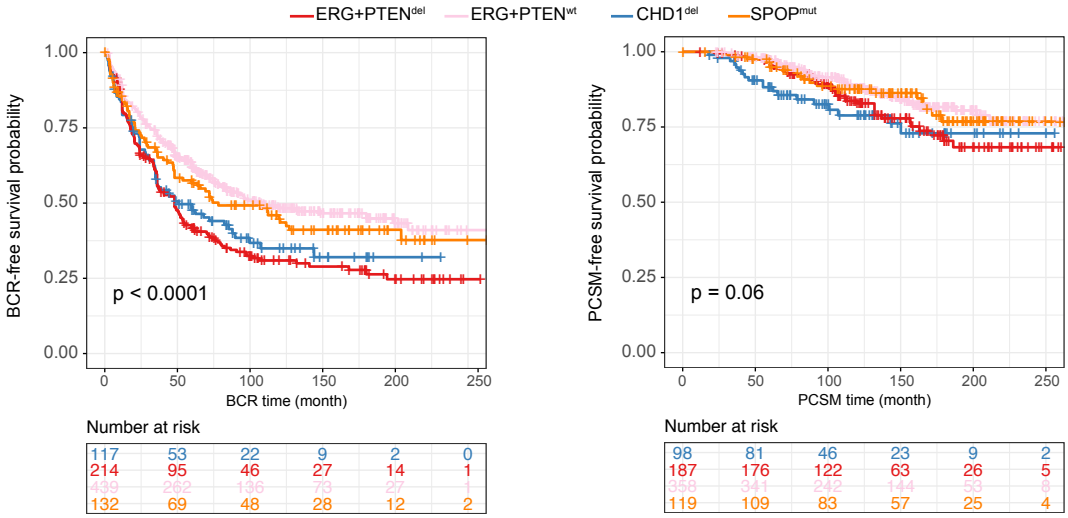

Figure S17. Prognostic outcome difference between late events of *PTEN* and *CHD1* deletions, and early events of *ERG* fusion and *SPOP* mutation via Kaplan-Meier analysis for biochemical recurrence (BCR) free and prostate cancer specific mortality (PCSM) free survival rates.

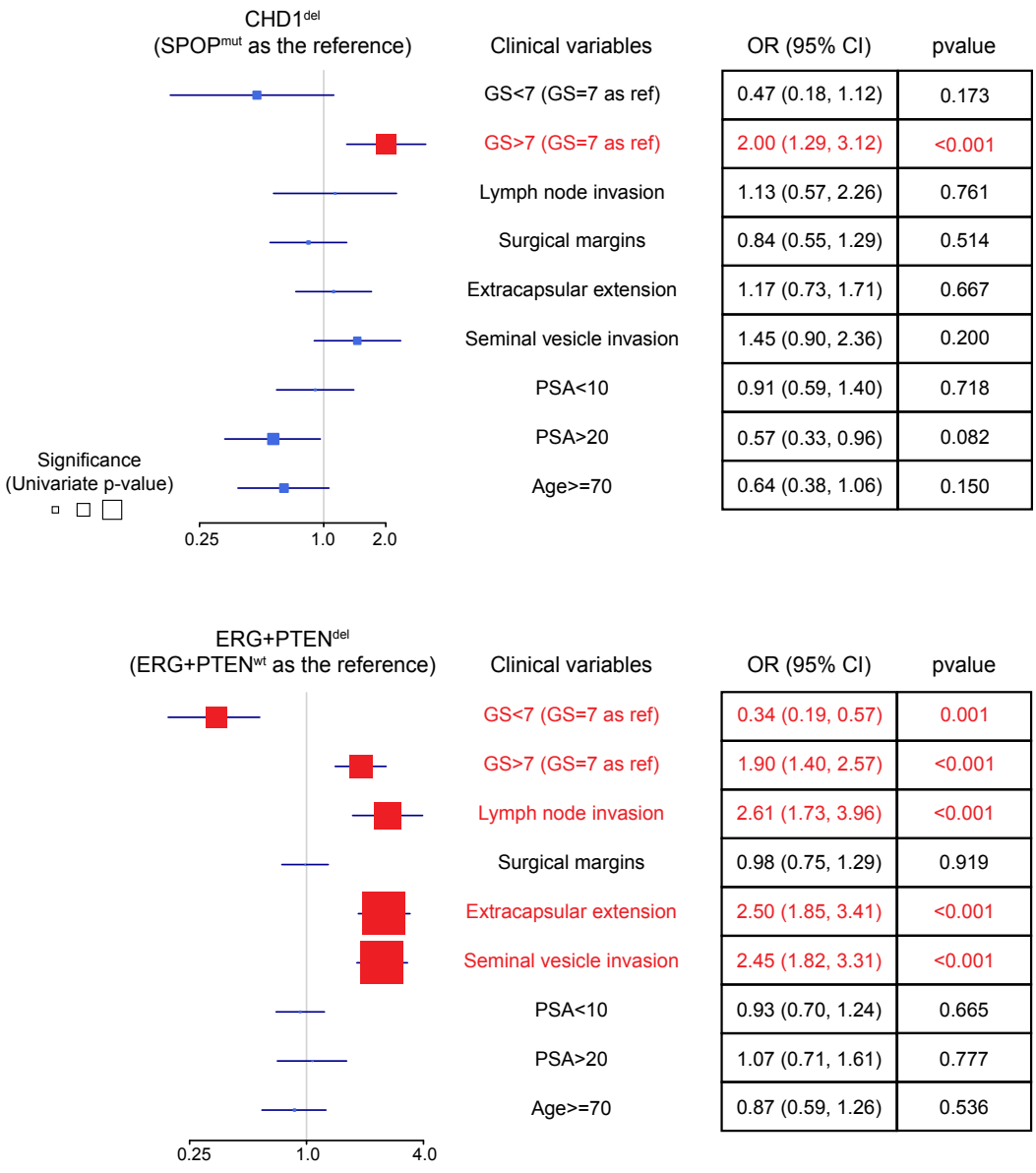

Figure S18. Pathological outcome difference between late and early event from each tumor lineage model in Decipher retrospective cohort (n=1,626) via univariable analyses.

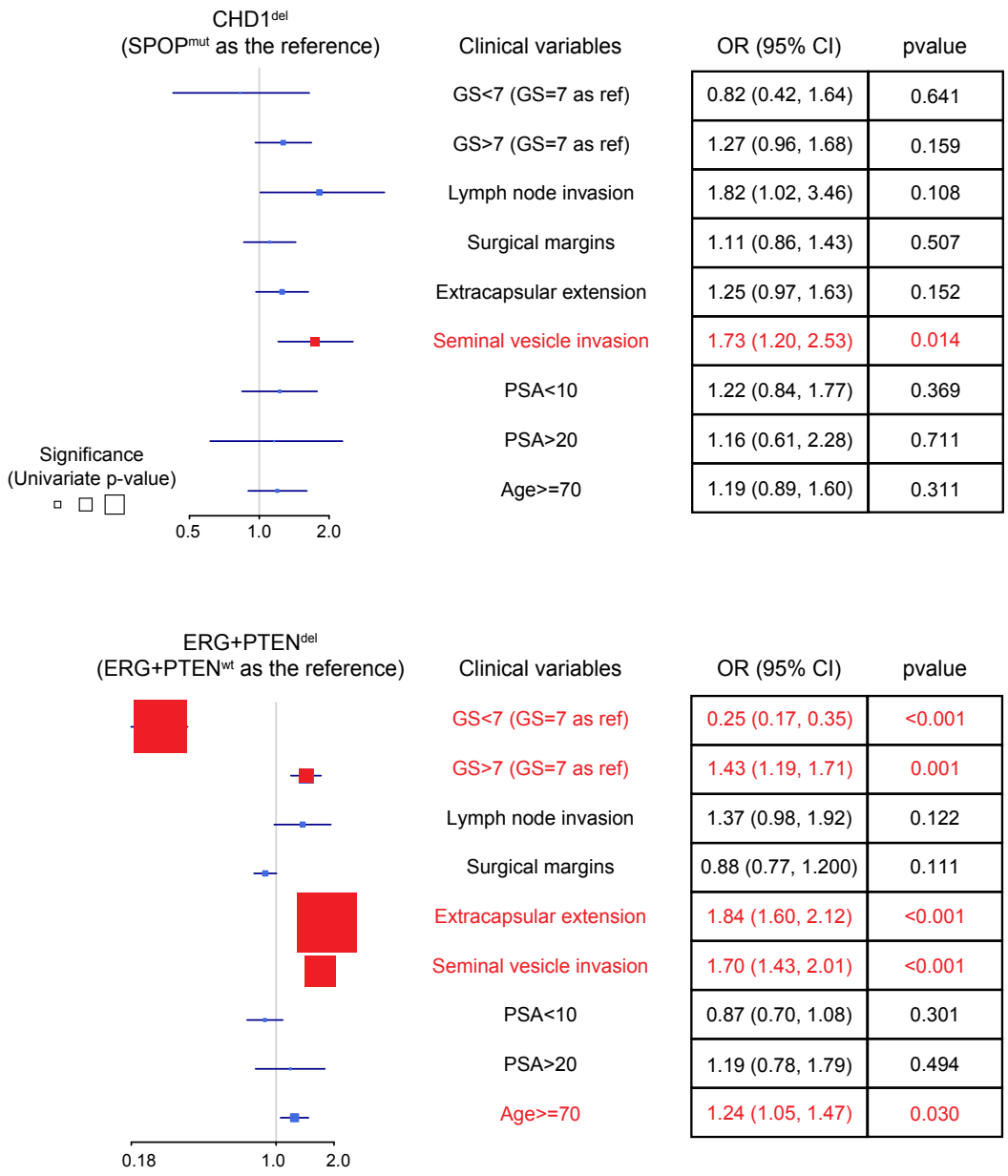

Figure S19. Pathological outcome difference between late events and early events in Decipher prospective cohort (n=6,532) via univariable analyses.

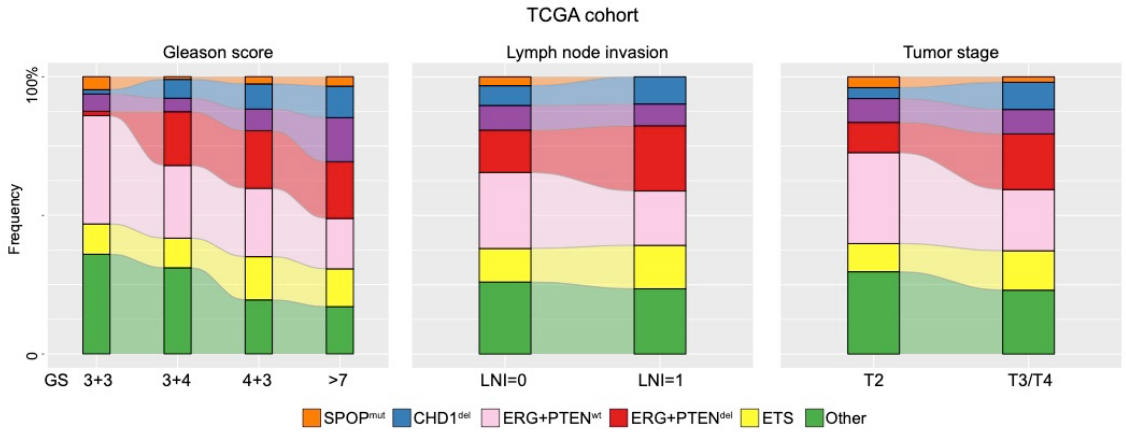

Figure S20. Alluvial diagrams of Gleason scores, lymph node invasion status and tumor stages from TCGA cohort.

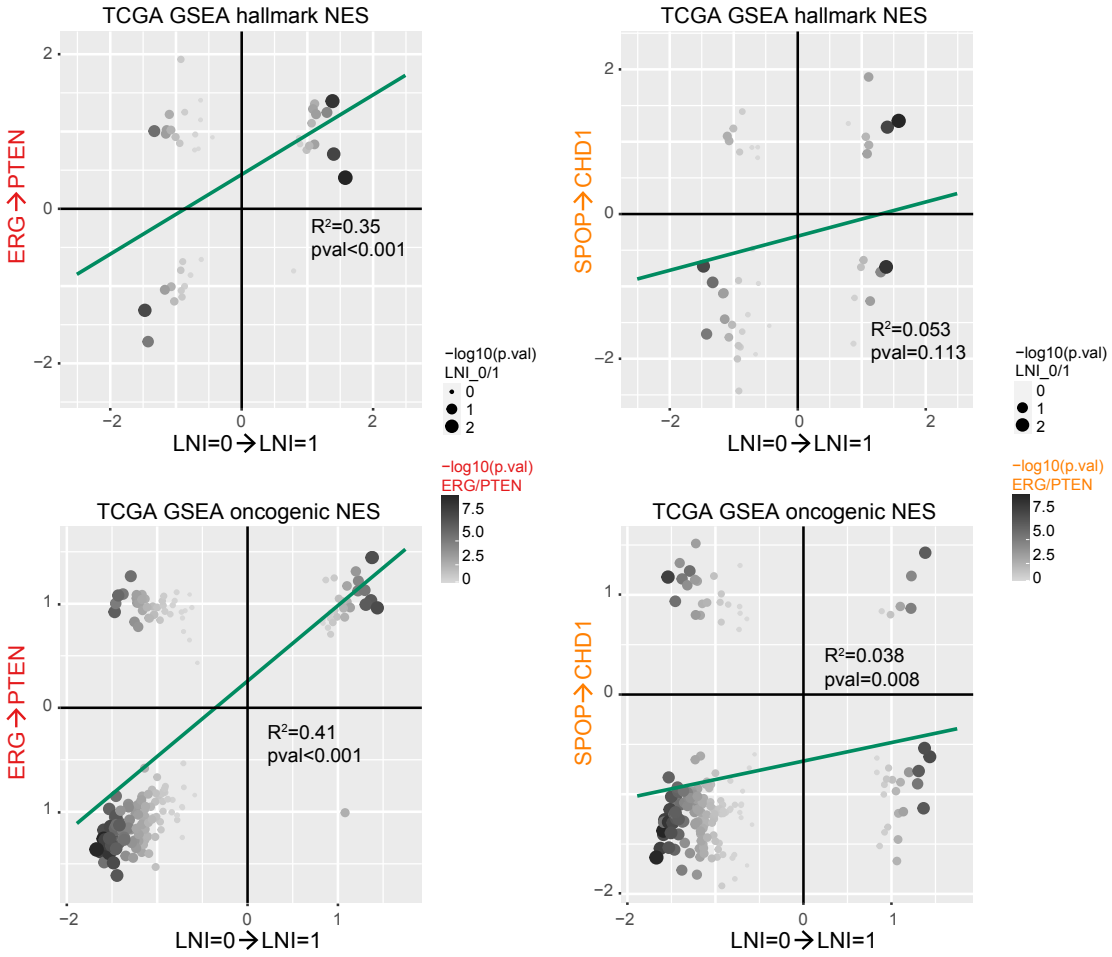

Figure S21. Correlation of gene set enrichment output between lymph node invasion and tumor lineages: similar signaling pathways between lymph node invasion and *ERG*/*PTEN* lineage (from the "early" to "late" state), but divergent pathways between lymph node invasion and *SPOP*/*CHD1* lineage.

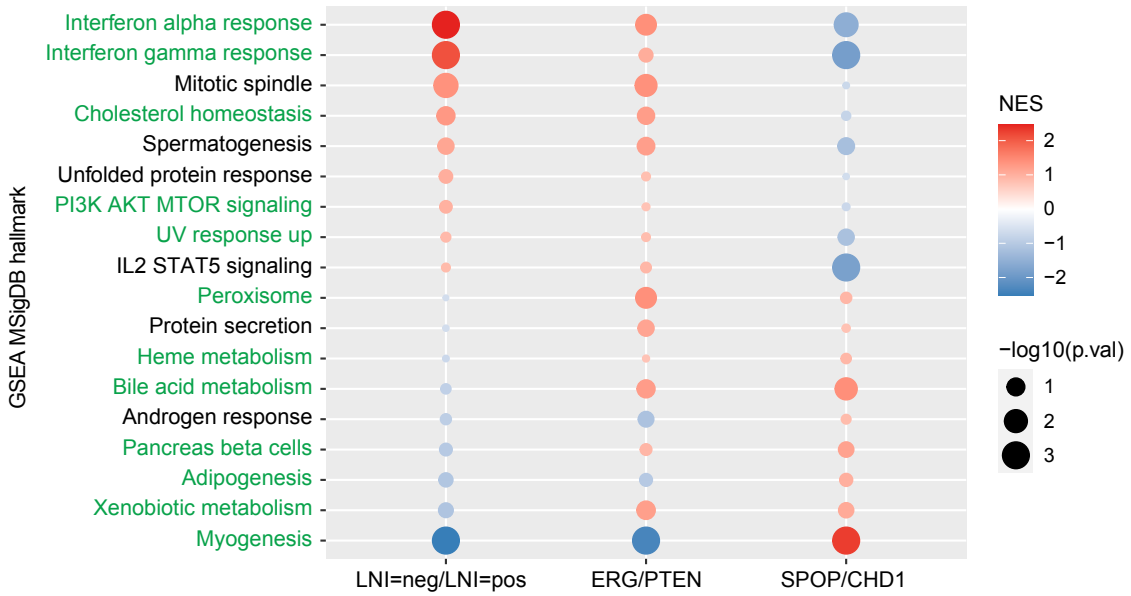

Figure S22. Divergent signaling pathways in *SPOP*/*CHD1* lineage, when compared to lymph node invasion (LNI) and *ERG*/*PTEN* lineage. NES represents normalized enrichment score from GSEA output. The significance of signaling pathway enrichment is shown by the size of the dots. Metabolism related pathways are labeled as green color.